Spectrochimica Acta Part A: Molecular and Biomolecular Spectroscopy 208 (2019) 315–324

Contents lists available at ScienceDirect

Spectrochimica Acta Part A: Molecular and Biomolecular Spectroscopy

journal homepage: www.elsevier.com/locate/saa

Absolute fundamental and overtone OH and OD stretching intensities of alcohols

Jens Wallberg, Henrik G. Kjaergaard*

Department of Chemistry, University of Copenhagen, Universitetsparken 5, Copenhagen Ø DK-2100, Denmark

ARTICLE INFO

Article history:
Received 5 July 2018
Received in revised form 21 September 2018
Accepted 25 September 2018
Available online 29 September 2018

Keywords:
Absolute intensity
Oscillator strength
Overtones
OH-stretch
OD-stretch
Cavity ring down
Gas-phase

ABSTRACT

Absolute intensities of the $\Delta v_{OH} = 1 - 2$ and $\Delta v_{OD} = 1 - 3$ transitions were determined for a range of alcohols (methanol, ethanol, 2-propanol, 1-propanol and tert-butanol) using conventional Fourier transform infrared (FTIR) spectroscopy. The intensities of the OH stretching transitions are stronger than the corresponding OD stretching transitions and become increasingly stronger with higher overtone transitions as expected from the reduced masses of the oscillators. Furthermore, accurate absolute intensities of the third and fourth OH stretching overtone transitions were determined using our newly constructed integrated cavity ring down (CRD) and FTIR spectrometer with experimental uncertainties generally less than 10%. The experiments were complemented by local mode calculations, with the potential energy surfaces and the dipole moment functions determined at the CCSD(T)/aug-cc-pVTZ level of theory. The calculated oscillator strengths of the $\Delta v_{OH} = 4 - 5$ transitions are within 25% of the experimental results.

1. Introduction

Vibrational stretching overtones have been suggested to impact photolytic reactions in the atmosphere. Photolysis of H_2SO_4 through overtone pumping of the OH stretch is a source of SO_2 at altitudes higher than 35 km [1-3] and similarly the photolysis of HNO_4 through pumping of the second and third OH-stretch overtones is thought to be a significant source of HO_x in the high latitude lower stratosphere [4,5]. The photolysis rate depends on the intensities of the vibrational overtone transitions and intensities of different overtone transitions in a range of atmospherically relevant species have been determined [2,3,5-7].

Studies of X—H stretching overtone intensities (where X is a heavy atom like O, N or C) have focused on the effect of the molecular structure near the X—H oscillator [8-13] and the agreement with calculated intensities, often within the local mode model [3, 14-22]. Whereas different experimental studies usually agree very well on the transition frequencies, with differences less than a percent, the intensities often vary significanly between different experimental studies [5,7,11,12]. One example is the third overtone transition of the OH stretch in ethanol where two different studies differed with more than 50% [11,12]. Furthermore, theoretical studies [23-28] have analyzed the properties of calculated oscillator strengths in greater detail and have proven to be an important tool as some of the atmospherically relevant compounds are difficult to measure [1]. However, calculated oscillator strengths at high level of theory such as QCISD and CCSD(T) are typically 30–50 % lower than the experimental values for the third and fourth overtones of stretching transitions[3,13,18,20,21].

Lange et al. [12] have previously reported experimental oscillator strengths of the $\Delta v_{OH} = 1 - 4$ transitions of alcohols in a study that expanded the work by Phillips et al. [11] who reported the oscillator strengths of the $\Delta v_{OH} = 3 - 4$ transitions in methanol, ethanol and 2-propanol as well as the oscillator strength of $\Delta v_{OH} = 5$ transition in methanol. Gas phase oscillator strengths of OD stretching transitions of the alcohols included in this study have, to our knowledge, not been reported.

We determine the oscillator strengths for the $\Delta v_{OH} = 1 - 2$ and $\Delta v_{OD} = 1 - 3$ transitions for a range of simple alcohols (methanol, ethanol, 1-propanol, 2-propanol and *tert*-butanol) using conventional FTIR spectroscopy. Furthermore, we determine the oscillator strengths for the $\Delta v_{OH} = 4 - 5$ using our newly constructed integrated CRD/FTIR setup. For ethanol and 2-propanol, we use our calculated intensities and experimental overtone bands to extract Boltzmann distributions between the conformers [29].

* Corresponding author.
E-mail address: hgk@chem.ku.dk (H.G. Kjaergaard).

https://doi.org/10.1016/j.saa.2018.09.046
1386-1425/

2. Experimental

2.1. Oscillator Strengths from FTIR Spectroscopy

The experimental oscillator strengths of the $\Delta v_{OH} = 1 - 2$ and $\Delta v_{OD} = 1 - 3$ were determined using conventional FTIR spectroscopy. The samples - methanol (MeOH, Sigma Aldrich, ≥99.9%), ethanol (EtOH, Sigma Aldrich, ≥99.8%), 2-propanol (2-PrOH, Sigma Aldrich, 99.5%), 1-propanol (1-PrOH, Labscan, ≥99.5%) and *tert*-butanol (*t*-BuOH, Sigma Aldrich, ≥99.5%) - and the deuterated samples - methan(ol-d) (MeOD, Sigma Aldrich, ≥99.5%D), ethan(ol-d) (EtOD, Sigma Aldrich, ≥99.5%D), 1-propan(ol-d) (1-PrOD, Sigma Aldrich, 99%D), 2-propan(ol-d) (2-PrOD, Sigma Aldrich, 98%D) and *tert*-butan(ol-d) (*t*-BuOD, Sigma Aldrich, 99%D) - were prepared on a glass vacuum line with a base pressure of 1×10^{-4} Torr. Sample flasks and an FTIR cell were fitted to the vacuum line with Ultra-Torr fittings (Swagelok). The samples were degassed by several freeze-pump-thaw cycles. An Agilent capacitance diaphragm (1×10^{-3}-10 Torr, CDG-500) pressure gauge was fitted directly to the FTIR cell. All FTIR spectra were recorded on the VERTEX 70 (Bruker) spectrometer with 1 cm^{-1} resolution and averaged over 500 scans. Fundamental OH and OD stretching transitions were recorded using a 10 cm static FTIR cell for all alcohols except 1-PrOH which was recorded with a 2.4 m static White cell (Infrared Analysis, Inc.). The spectra were recorded using a liquid nitrogen-cooled Mercury Cadmium Telluride (MCT) detector and a mid-infrared (MIR) light source. The spectra of the first overtones were recorded using a 6 m static White cell (Infrared Analysis, Inc.) for the OH stretching transitions and a 4.8 m static White cell (Infrared Analysis, Inc.) for the OD stretching transitions with a near-infrared (NIR) light source and an Indium Gallium Arsenide (InGaAs) detector. The second overtone of the OD stretching transitions was recorded using a 16 m static White cell (Infrared Analysis, Inc.) with a NIR light source and an InGaAs detector. All OH stretching transitions were recorded using a CaF_2 beamsplitter and all OD stretching transitions were recorded using a KBr beamsplitter. Spectra were recorded with different pressures and the integrated absorbances, $\int A(\tilde{\nu})d\tilde{\nu}$, were determined by integration of the whole band with a straight base line using the Integration Gadget in OriginPro 2016. Pressures were kept below 30 Torr to avoid significant dimerization [30]. The oscillator strengths, f_{FTIR}, were determined from the slope of a linear fit of integrated absorbances versus the pressure from [14,16,31]:

$$\int A(\tilde{\nu})d\tilde{\nu} = \frac{f_{FTIR} \times l}{2.6935 \times 10^{-9} \quad K^{-1} \quad Torr \quad m \quad cm \times T} \times p, \qquad (1)$$

where T is the temperature, p is the pressure and l is the optical path length.

For the oscillator strengths determined using the static FTIR setup, several factors contribute to the reported uncertainties. Firstly, there is a statistical uncertainty arising from the fit of pressures and integrated absorbances according to Eq. (1). For the fundamental and first overtone of the OH and OD stretching transitions the statistical uncertainty (defined as 95% confidence interval from a two-tailed *t* test) was below 6% in all cases. The spectra of the $\Delta v_{OD} = 3$ transitions have worse signal-to-noise ratios than the fundamental and first overtone transitions and the statistical uncertainties are significantly higher (<22%). Additional sources of uncertainty come from the accuracy of our thermometer and pressure gauge, the uncertainty of the optical path length of our cells as well as condensation of our sample on the surfaces of our cells. Condensation has previously been shown to be an important factor that could cause experimental oscillator strengths to be underestimated by at least 50% [13]. We monitor the condensation by recording the 500 scans in fractions of 100 scans each and exclude measurements with significant condensation. Lastly, the choice of integration range for the absorption band might introduce biases. For a single transition with a strictly flat baseline, the integrated absorbance should converge to a single value as the integration range is expanded. We test our choice of integration range by systematically changing the range and analysing the convergence properties of the resulting integrated absorbances (see section S18 in the SI for further discussion). We estimate that the cumulative effect on the non-statistical uncertainties is less than 5% which we include in the reported uncertainties.

2.2. Integrated CRD/FTIR Flow Setup

We determine the experimental oscillator strengths for the $\Delta v_{OH} = 4 - 5$ transitions using our newly constructed integrated CRD/FTIR flow setup. The samples are introduced into the spectrometers by bubbling nitrogen through the liquid phase. The flow goes through a 10 cm cell mounted in an FTIR spectrometer before entering the CRD flow cell. The partial pressure of the sample is determined from the FTIR spectra.

The laser system used for our CRD setup is a tunable nanosecond laser system from EKSPLA (NT342B-20-SH/SFG-AW-H/2H) containing both a pump laser (NL300 series laser) and an OPO system. A 1064 nm laser pulse from its Q-switched Nd:YAG laser is frequency tripled to 355 nm and the ~ 100 mJ pulse is directed into the OPO system consisting of two OPO crystals (type 2 BBO crystal). The resulting OPO laser pulse is 3–5 ns long and has a linewidth of $< 5\ cm^{-1}$. The pulse energy depends on the wavelength and has a peak value of ~ 30 mJ at 450 nm.

Absorption cross sections are underestimated in a CRD spectrum if the linewidth of the laser is comparable to the width of the spectral band [32-34]. However, integrated cross sections are less sensitive to this bandwidth effect [34] and due to the generally broad nature (at room temperature and atmospheric pressure) of vibrational overtones in larger molecules, like the ones investigated here, absolute intensities of these transitions can be determined reliably.

The optical layout of the setup is shown in Fig. 1. The laser pulse from the OPO-laser is guided through a series of different optics by two aluminium mirrors (Thorlabs, PF05-03-F01) before being introduced to the cavity: the focusing lens (Thorlabs, LA4184) with a focal length of 50 cm ensures that the diameter of the pulse is similar to the TEM_{00} transverse modes of the cavity. The combination of a polarizer (Thorlabs, GL10-A) and a quarter wave plate (Thorlabs, AQWP05M-600) makes an optical insulator that protects the laser from back-reflections of the laser pulse. Lastly, neutral density filters (Thorlabs, NEK02) are installed in order to remove excess energy of the pulse if the PMT signal is saturated.

Custom made CRD mirrors from Layertec centred around 755 nm (coating no. 127183 with $R > 99.99\%$ in the 735–790 nm range, peak reflectivity 99.9935%) for $\Delta v_{OH} = 4$ transitions and 610 nm (coating no. 134700, with $R > 99.99\%$ in the 590–625 nm range) for $\Delta v_{OH} = 5$ transitions are used. The radius of curvature of the mirrors are 100 cm and with a cavity length of 97 cm we can achieve a stable cavity [33]. The mirrors were placed in custom made bellow mirrors mounts designed by Brown and co-workers [35] and are purged to avoid condensation of sample on the mirrors. The bellow mirror mounts are placed in 1" mirror mounts (Newport, U100-A3K).

The detector is a photomultiplier tube (PMT) module (Hamamatsu, H9433-201) with a frequency bandwidth of 10 MHz which is powered by a commercial power supply (Hamamatsu, C10709). The signal output of the PMT is connected to a 14-bit data acquisition card (National Instruments, PCI-6132 S Series Multifunction DAQ) through a shielded BNC connector block (National Instruments, BNC-2110).

The setup is controlled by our own LabVIEW based software. The software reads every single ring down signal from the DAQ and selects the reliable part of the ring down by excluding parts of the ring down signal above the manufacturers recommendations for the

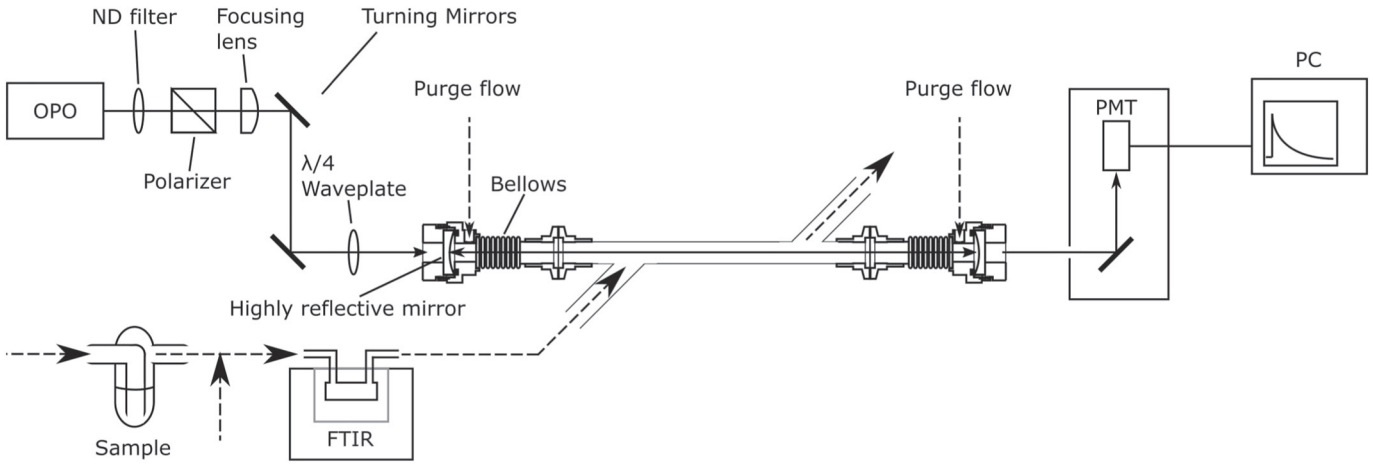

Fig. 1. The design of the CRD setup.

PMT (3V) and lower than the noise level. The reliable part of the ring down is transformed to a ln(intensity) versus time plot to determine the ring down time, τ. The slope of the plot (τ^{-1}) is determined from a unweighed linear least square fit performed using LabVIEWs Linear Fit VI. We increase the spectral signal-to-noise ratio by averaging the determined τ's for multiple ring downs at each wavelength.

We determine the absorption coefficient, α, using the relationship [36]:

$$\alpha = \frac{R_l}{c}\left(\frac{1}{\tau} - \frac{1}{\tau_0}\right), \tag{2}$$

where c is the speed of light and $R_l = l/l_s$ with l being the distance between the mirrors, l_s the effective distance over which the sample is present and τ and τ_0 is the ring down time with and without sample, respectively.

We determine R_l experimentally using the broad $\Delta v_{CH} = 5$ stretching transition in propane [14] to be 2.78 for the specific combination of purge flow rates and sample flow rates used in this study. We have recorded the spectra shown in Fig. 2 (a) of this transition under two circumstances. First, we record a spectrum of a diluted propane mixture introduced into the sample flow (case 1). Secondly, we record a spectrum where the diluted propane mixture is used as both sample flow and purge flow (case 2). In the second case, $R_l = 1$ and since the number density of propane is the same in the two cases, the R_l value for our regular flow setup can be determined from a plot of absorption coefficients covering the entire band:

$$\alpha'_2 = R_l \alpha'_1, \tag{3}$$

with α'_2 and α'_1 being defined as $\alpha' = \frac{1}{c}\left(\frac{1}{\tau} - \frac{1}{\tau_0}\right)$ for case 2 and case 1, respectively. We use α' values for wavenumbers covering the entire band and we show the plot in Fig. 2 (b). In section S3 of the SI, we show the derivation of Eq. (3) and demonstrate that it is important for the determination of R_l to use a broad transition. We demonstrate this by determining R_l from the A-band in molecular oxygen (the $b^1\Sigma_g^+(v' = 0) \leftarrow X^3\Sigma_g^-(v'' = 0)$ transition). The narrow and clearly separated rotational lines in the A-band results in an underestimation of the absorptivity and R_l due to the laser bandwidth effect [32-34].

The detection limit of our setup was calculated to be $5 \times 10^{-10}\text{cm}^{-1}$ in the third OH stretching overtone region and $8 \times 10^{-10}\text{cm}^{-1}$ in the fourth OH-stretching overtone region when averaging over 100 ring downs using the relationship [36]:

$$\alpha_{min} = \frac{R_l}{c}\frac{\Delta\tau_0}{\tau_0^2}, \tag{4}$$

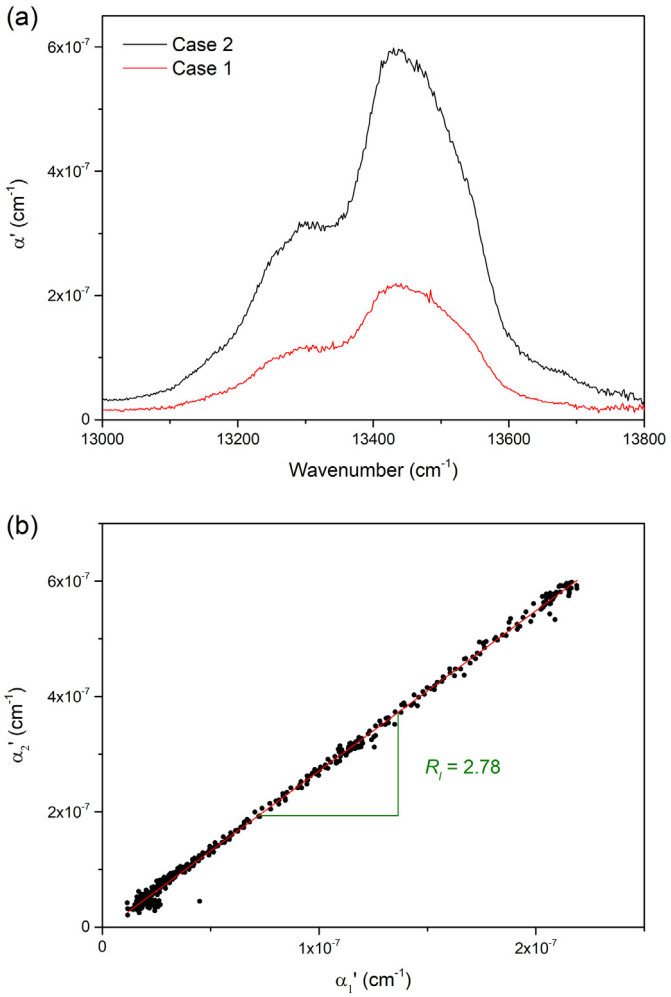

Fig. 2. (a) Spectra of the $\Delta v_{CH} = 5$ stretching transition in propane for the two cases described in the text used for determining R_l. (b) The absorption coefficients for case 2 plotted against case 1 according to Eq. (3).

where $\Delta\tau_0$ is the uncertainty in τ_0. Our detection limits are comparable to the detection limits for other pulsed CRD setups [3,7]. For molecules with overtone cross sections similar to sulphuric and nitric acid [3,7] this corresponds to a detection limit of 3×10^{-4} Torr and 5×10^{-3} Torr for the third and fourth OH-stretching overtone, respectively.

2.3. Oscillator Strengths of Overtone Transitions using CRD

The samples were placed in the sample holder of the CRD setup and used without further purification. The sample flow was generated by bubbling N_2 (25–200 SCCM) through the liquid phase and subsequently mixing it with pure N_2 to achieve a total sample flow of 500 SCCM (standard cubic centimetre per minute). By changing the mixing ratio (while maintaining the same total sample flow) different partial pressures of the sample were achieved. See section S2 in the SI for further details about the flow setup.

The partial pressure of the sample was determined spectroscopically by measuring the intensity of the band associated with the fundamental OH stretching transition (with FTIR) while concurrently recording the overtone spectrum (with CRD). The sample flow was initially led through a 10 cm flow cell placed in an FTIR (VERTEX 80, Bruker) spectrometer and subsequently through the CRD cell as illustrated in Fig. 1. Spectra of the fundamental OH stretching transition were recorded continuously (with a MCT detector, MIR light source, 1 cm^{-1} resolution and 100 scans) as the CRD was scanning to monitor potential changes in the partial pressure. If a significant drift in the partial pressure was observed during a wavelength scan, the overtone spectrum was discarded. Five FTIR spectra recorded during an overtone CRD scan were averaged and used for the final determination of the partial pressure of alcohol in the flow.

The overtone CRD spectra were recorded with a step size of 0.1 nm (corresponding to $\sim 1.8\ cm^{-1}$ for $\Delta v_{OH} = 4$ and $\sim 2.8\ cm^{-1}$ for $\Delta v_{OH} = 5$) with 100 ring downs being recorded and averaged at each wavelength step. The control voltage of the PMT was set to 0.250 V and the sampling rate was 2 MHz. We use ND filters, placed between the laser and the polarizer, to avoid saturation of the PMT signal. For the $\Delta v_{OH} = 4$ region a ND filter with an optical density of 2.0 was used for MeOH, EtOH and 2-PrOH and no ND filter was used for 1-PrOH and *t*-BuOH. For the $\Delta v_{OH} = 5$ transitions a ND filter with an optical density of 0.5 was used for *t*-BuOH and an optical density of 1.0 for the remaining alcohols.

The oscillator strength of the overtone transition, $f_{overtone}$, was determined from the slope of a linear fit of the integrated absorptivity of the overtone transition, $\int \alpha_{CRD}(\tilde{\nu})d\tilde{\nu}$, versus the integrated absorbance of the fundamental transition, $\int A_{FTIR}(\tilde{\nu})d\tilde{\nu}$, determined at different partial pressures of sample:

$$\int \alpha_{CRD}(\tilde{\nu})d\tilde{\nu} = \frac{f_{overtone}}{f_{\Delta v_{OH}=1}} \frac{\ln(10)}{l_{FTIR}} \int A_{FTIR}(\tilde{\nu})d\tilde{\nu}, \quad (5)$$

where l_{FTIR} is the optical path length of the FTIR cell and $ln(10)$ is accounting for α being in log e base and A being in log 10 base (see section S1 of the SI). We use our experimentally determined oscillator strengths of the fundamental transition, $f_{\Delta v_{OH}=1}$, reported in this paper. Both the fundamental spectra and the overtone spectra were integrated using the Integration Gadget in OriginPro 2016. In section S12 of the SI we demonstrate that the method is insensitive to the choice of FTIR absorbance band. We find good agreement between oscillator strengths of the $\Delta v_{OH} = 4$ transitions obtained by using either the $\Delta v_{OH} = 1$ or the $\Delta v_{CH} = 1$ band to determine the partial pressure.

For the $\Delta v_{OH} = 4 - 5$ transitions recorded using the CRD/FTIR flow setup, we have different sources of experimental uncertainties than for the transitions recorded using the static FTIR setup. Firstly, we have a statistical uncertainty (defined as 95% confidence intervals from a two-tailed *t* test) from the fits of the $\int \alpha_{CRD}(\tilde{\nu})d\tilde{\nu}$ and $\int A_{FTIR}(\tilde{\nu})d\tilde{\nu}$ according to Eq. (5). Furthermore, we have the uncertainty from the determination of R_l as well as the uncertainty for $f_{\Delta v_{OH}=1}$. The cumulative uncertainties for these three sources are less than 15% (3–12 %). Analogous to the oscillator strengths determined using the static FTIR setup, there are additional uncertainties from choice of integration range and fluctuations in the partial pressure of our sample in the flow. We validate our choice of integration range using the method described for the oscillator strengths determined using our static FTIR setup. As mentioned previously, we monitor the partial pressure of our sample during the recording of the overtone spectra and exclude measurements with significant drifts in partial

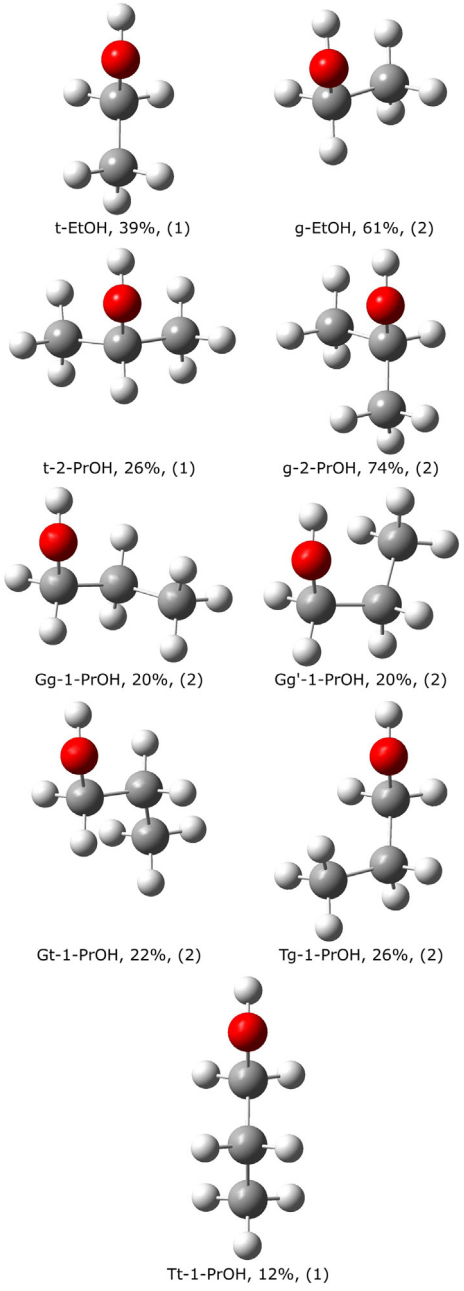

Fig. 3. Conformers of EtOH, 2-PrOH and 1-PrOH with Boltzmann distribution and structural degeneracy in brackets. The Boltzmann distribution was calculated using CCSD(T)/aug-cc-pVTZ electronic energies and B3LYP/aug-cc-pVTZ thermal corrections. Boltzmann distributions of the conformers of EtOD, 2-PrOD and 1-PrOD are within 0.5% of the Boltzmann distributions of the non-deuterated species.

pressure. Lastly, we assume that the oscillator strengths are independent of the total pressure. Lange et al. showed that the oscillator strengths are approximately independent of pressure as they found the effect of pressure broadening on the oscillator strengths to be less than 3% [12]. We estimate that the additional cumulative effect of these three sources of uncertainty is less than 5% which we include in the reported uncertainties giving us total uncertainties less than 14%.

3. Computational

Methanol and *tert*-butanol have one unique conformer whereas ethanol and 2-propanol each have two unique conformers and 1-propanol has five conformers [26]. The fractional gas-phase equilibrium populations of these conformers, $F(M)$, were calculated according to the Boltzmann distribution:

$$F(M) = \frac{g_M \exp(-G_M^{\ominus}/RT)}{\sum_i g_i \exp(-G_i^{\ominus}/RT)} \quad (6)$$

where g is the degeneracy, G is the Gibbs energy relative to the lowest energy conformer, R is the gas constant, T is the absolute temperature and i spans all the unique conformers. All conformers were optimized with the B3LYP [37,38] functional and aug-cc-pVTZ basis set [39] using the keywords opt=tight and int=ultrafine in Gaussian09 [40]. The conformers were subsequently reoptimized at CCSD(T)/aug-cc-pVTZ level of theory [41,42] with MOLPRO 2012.1 [43]. Threshold criteria for the optimization procedure were: energy=1 × 10^{-8} a.u., gradient=1 × 10^{-6} a.u. and step=1 × 10^{-8} a.u. Threshold criteria for the energy calculations were: energy=1 × 10^{-9} a.u., orbital= 1 × 10^{-8} a.u. and coeff=1 × 10^{-8} a.u. The Gibbs energies were calculated using the CCSD(T)/aug-cc-pVTZ electronic energies and the B3LYP/aug-cc-pVTZ thermal corrections.

The calculated oscillator strength of a vibrational transition is given by [14,31]:

$$f_{v\leftarrow 0} = 4.702 \times 10^{-7} \mathrm{cmD}^{-2}\ \tilde{\nu}_{v\leftarrow 0} |\vec{\mu}_{v\leftarrow 0}|^2 \quad (7)$$

where $\tilde{\nu}_{v\leftarrow 0}$ is the transition frequency and $\vec{\mu}_{v\leftarrow 0} = \langle v|\vec{\mu}|0\rangle$ is the transition dipole moment. All energies and dipole moments used for vibrational calculations are calculated at CCSD(T)/aug-cc-pVTZ level of theory with the same threshold criteria as for the optimizations. The dipole moments were calculated with the finite field approach with an applied field of ±0.0001 a.u. OH stretching frequencies

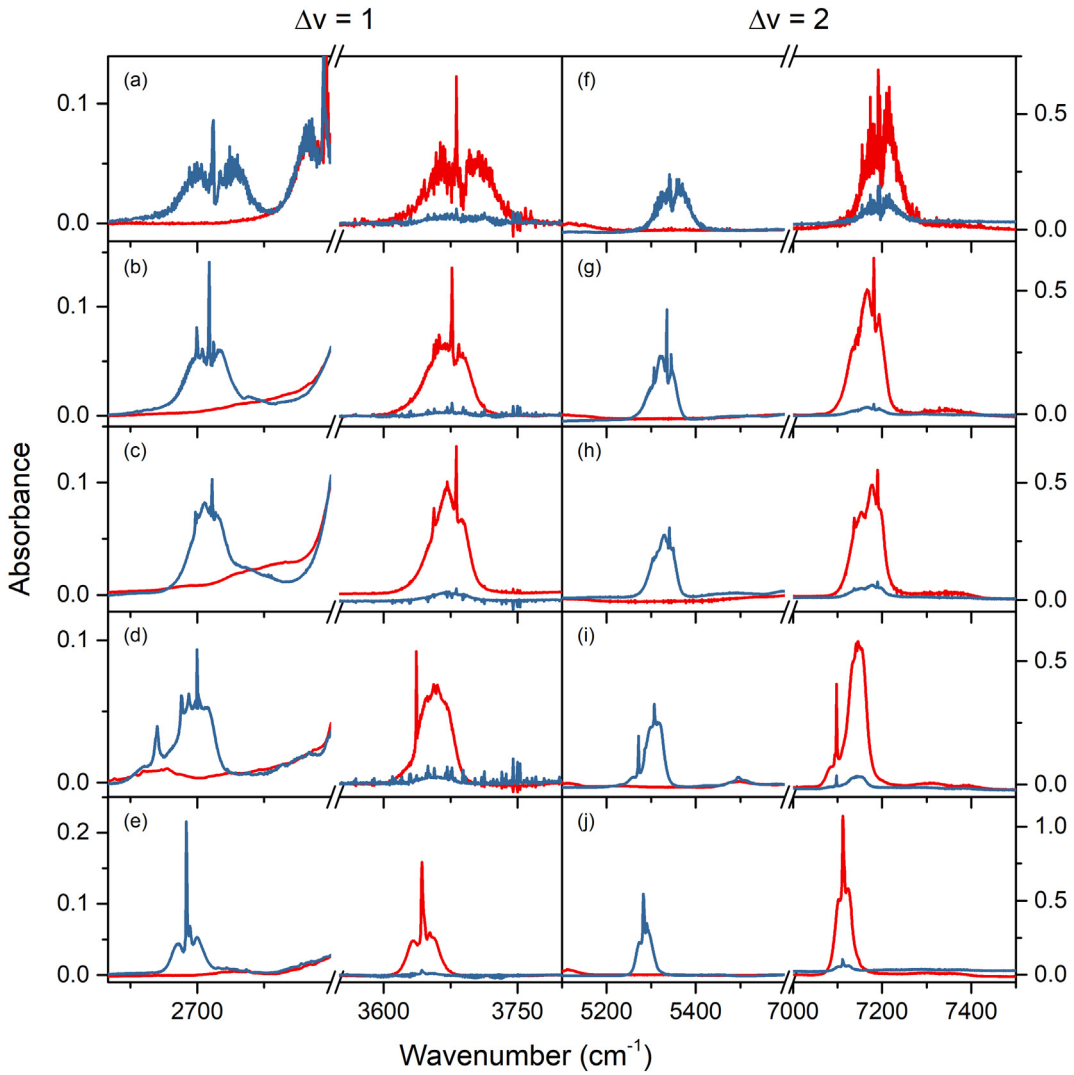

Fig. 4. FTIR spectra of the fundamental and first overtone OH and OD stretching transition of the five alcohols. (a)–(e): Spectra of the $\Delta v_{OH} = 1$ and $\Delta v_{OD} = 1$ regions for the non-deuterated (red) and deuterated (blue) alcohols. (f)–(j): Spectra of the $\Delta v_{OH} = 2$ and $\Delta v_{OD} = 2$ regions for the non-deuterated (red) and deuterated (blue) alcohols. (a)+(f): Methanol, (b)+(g): Ethanol, (c)+(h): 1-Propanol, (d)+(i): 2-Propanol, (e)+(j): *tert*-Butanol. Spectra recorded with a pressure of 8–10 Torr.

and intensities for all five molecules were calculated with a one-dimensional local mode (1D LM) model [44,45]. In our 1D local mode model [44,45] the potential energy surface of the OH stretch is represented by a spline fit generated from points obtained by displacing the OH bond from −0.40 Å to 0.70 Å in steps of 0.05 Å and the Schrödinger equation is solved numerically [44,45]. The dipole moment is expanded as a Taylor series to sixth order, with the expansion coefficients determined by fitting a 6th order polynomial to a set of dipole moments calculated at the same displacements as the PES. For the molecules with multiple conformers, the reported oscillator strengths are a Boltzmann weighted sum of oscillator strengths for the individual conformers, which are given in section S6 of the SI.

4. Results and Discussion

4.1. Conformers and Boltzmann Distribution

In Fig. 3 we show the different conformers of EtOH, 2-PrOH and 1-PrOH along with their Boltzmann distributions. Boltzmann distributions of the conformers of EtOD, 2-PrOD and 1-PrOD are within 0.5% of the Boltzmann distributions of the non-deuterated species. The conformers of a given molecule are named with respect to one or two dihedral angles where *gauche* (g) refers to a dihedral angle of ∼60° and *trans* (t) refers to a dihedral angle of ∼180°. The two conformers of EtOH are defined according to the HOCC dihedral angle and 2-PrOH according to the HOCH dihedral angle with the latter hydrogen being the hydrogen covalently bonded to the central carbon atom. For 1-PrOH two dihedral angles are needed. The first (capital) letter refers to the HOCC dihedral angle and the second letter refers to the OCCC dihedral angle. The prime in the Gg' conformer of 1-PrOH indicates that the OCCC dihedral angle is ∼ -60°. The Boltzmann distributions are in good agreement with previous results by Takahashi et al. [26] obtained at B3LYP/6-311++G(3df,3pd) level of theory. Our calculated energy differences between the *trans* and *gauche* conformers of EtOH and 2-PrOH are within the range of experimentally determined energy differences. For EtOH the experimental energy difference is 40 cm^{-1} to 245 cm^{-1} [46-48] and for 2-PrOH the experimental energy difference 87 cm^{-1} to 158 cm^{-1} [49,50], which compares reasonably with our calculated energy differences of 50 cm^{-1} and 70 cm^{-1} for EtOH and 2-PrOH, respectively.

4.2. Spectra

The spectra of the $\Delta v_{OH} = 1 - 2$ and $\Delta v_{OD} = 1 - 2$ stretching transitions are shown in Fig. 4. Our spectra of $\Delta v_{OH} = 1 - 2$ only show negligible contamination of water. The $\Delta v_{OD} = 1$ transitions overlap with the low energy tail of the $\Delta v_{CH} = 1$ transitions which we subtract from the OD spectra using the spectra of the non-deuterated alcohols as references (see S13 in the SI for further discussion). The spectra of the deuterated alcohols show minor impurities of the non-deuterated alcohols which is most clearly seen from the absorption features in the $\Delta v_{OH} = 1$ and $\Delta v_{OH} = 2$ stretching regions. The measured pressures are corrected for the partial pressures of the non-deuterated alcohol which we determine

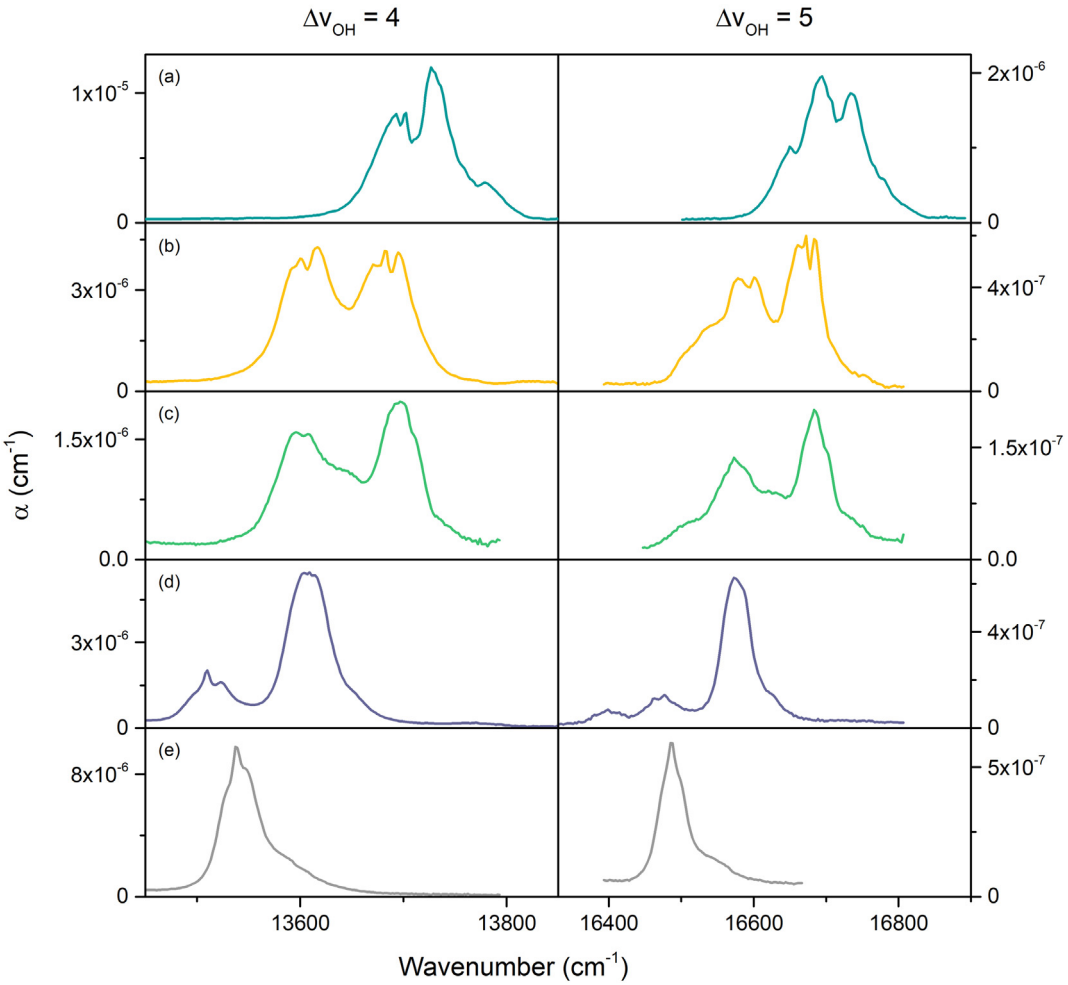

Fig. 5. CRD spectra of the $\Delta v_{OH} = 4$ and $\Delta v_{OH} = 5$ transitions in the five alcohols: (a) Methanol, (b) Ethanol, (c) 1-Propanol, (d) 2-Propanol, (e) *tert*-Butanol.

spectroscopically from the integrated absorbance of the OH stretching transition and its experimental oscillator strength. For the determination of the oscillator strengths of the $\Delta v_{OD} = 1$ stretching transitions we use the $\Delta v_{OH} = 1$ stretching transitions to correct our measured pressures and for the determination of the oscillator strengths of the $\Delta v_{OD} = 2 - 3$ stretching transitions we use the $\Delta v_{OH} = 2$ stretching transitions.

The spectra of the third and fourth overtone regions of the OH stretch for the five alcohols are shown in Fig. 5. The two different conformers of EtOH and 2-PrOH are clearly resolved in both regions. For 1-PrOH, the transition frequencies of the five conformers are too close to be resolved. The rotational structure of the overtone transitions can only be partially resolved due to the linewidth of our laser ($< 5 cm^{-1}$). As an example, the spectra of MeOH could indicate that multiple transitions are present, however, comparison to higher resolution spectra [51] reveals that the dominating structures are the P and R branches with the Q-branches being absent from the spectra.

The spectra of the fourth overtone transitions are more complicated than the third overtone region due to coupling of the OH to the CH oscillator in *trans* position, which previously has been studied by isotopic substitution in e.g. MeOH, EtOH, 2-PrOH and formic acid [52-57]. This coupling is perhaps most clearly seen in the fourth overtone spectrum of 2-PrOH that contains three spectrally resolved bands. The lowest energy transition has been assigned to a combination band involving the OH and CH oscillators in resonance with the $\Delta v_{OH} = 5$ transition of *t*-2-PrOH [52,53]. The resonance coupling transfers intensity from the $\Delta v_{OH} = 5$ bands to the combination bands converting the latter from an effectively "dark" state to a "bright" state and we assign all intensity in these regions to the OH stretching oscillators. The combination band do contribute slightly to the total intensity and we assess the error introduced by ignoring this contribution from previous calculations on formic acid [57]. These calculations show that intensity of combination band without the resonance coupling would be approximately a factor of 70 weaker than the $\Delta v_{OH} = 5$ transition which is negligible compared to our experimental uncertainties.

The spectra shown in Fig. 5 have excellent signal to noise ratios (S/N=74-338). We estimate that our setup (with mirrors of similar reflectivity compared to our current mirrors) could record spectra up to $\Delta v_{OH} = 7$ for compounds with vapor pressures similar to those of the alcohols in this study.

There is a good agreement between our transition frequencies and the transition frequencies reported previously [48, 51-53, 56] with the largest difference being $8 cm^{-1}$ and most differences being smaller than the linewidth of our laser.

4.3. OH and OD Stretching Intensities

The oscillator strengths of the $\Delta v_{OH} = 1 - 5$ and the $\Delta v_{OD} = 1 - 3$ transitions are shown in Fig. 6 (a) and listed in Table 1 along with the experimental uncertainties discussed in the experimental section.

For the fundamental transitions, there seems to be a quite clear trend in the oscillator strengths which are ordered according to whether the alcohol group is attached to a primary, secondary or tertiary carbon, i.e. the ordering of the oscillator strengths are: MeOH > EtOH ≃ 1-PrOH > 2-PrOH > *t*-BuOH (with the same trend for the deuterated alcohols). However, this trend is gradually lost through the overtones. For the fundamental transitions the difference between the oscillator strengths of methanol and *tert*-butanol is more than a factor of 2, which is decreased to a factor of 1.3 in the first overtone for both the OH and OD stretching transitions. For higher overtones the differences in intensities among the alcohols do not exceed the experimental uncertainties. For the $\Delta v_{OH} = 4 - 5$ stretching transitions, the oscillator strengths are all within 15% of the average values of 2.0×10^{-9} and 1.9×10^{-10} for the $\Delta v_{OH} = 4$ and $\Delta v_{OH} = 5$ stretching transitions, respectively. The small variances in oscillator strengths for the high overtone transitions are similar to previous studies [8-10].

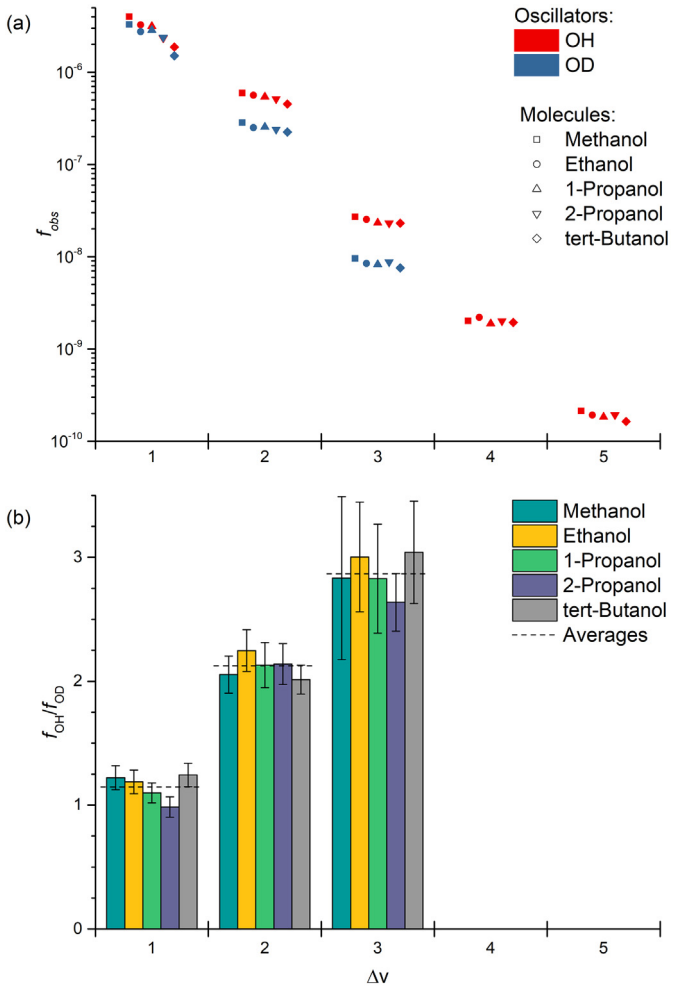

Fig. 6. (a) Experimental oscillator strengths and (b) ratios of experimental oscillator strengths for OH to the OD transitions. The oscillator strengths for $\Delta v_{OH} = 3$ are taken from Ref. [12].

We show the experimental ratios between oscillator strengths of the OH stretching transitions relative to the OD stretching transition (f_{OH}/f_{OD}) in Fig. 6 (b). Across the series of alcohols in this study, we find that the f_{OH}/f_{OD} ratios are approximately the same for a given transition (Δv) which is also indicated in Fig. 6 (b). The f_{OH}/f_{OD} ratios increase with increasing vibrational quantum number.

The oscillator strength of a transition depends on the transition frequency and the transition dipole moment as shown in Eq. (7). In section S16 of the SI, we analyse the theoretical f_{OH}/f_{OD} ratio and show that it can be greatly simplified through a couple of approximations. One key approximation in the simplification is the harmonic oscillator approximation. Under the harmonic oscillator approximation, the overlap integrals of the transition dipole moment expansion only depend on the reduced masses and the force constants (i.e. the second derivative of the potential energy surface). Since the potential energy surface of an OH stretching vibration is identical to the potential energy surface of the corresponding OD stretching vibration, the force constants cancel and the simplified equation depend only on the reduced masses of the OH and OD oscillator, respectively, as well as the change in vibrational quantum number of the transition (Δv): $\frac{f_{OH}}{f_{OD}} \approx \left(\frac{\mu_{OD}}{\mu_{OH}}\right)^{\frac{\Delta v+1}{2}}$. This simplification overestimates the f_{OH}/f_{OD} ratios but does qualitatively explain the increase with Δv.

Table 1
Experimental[a] and calculated[b] oscillator strengths of the OH and OD stretching overtone transitions.

		Δv				
		1 ($\times 10^{-6}$) [c]	2 ($\times 10^{-7}$) [c]	3 [d] ($\times 10^{-8}$) [c]	4 ($\times 10^{-9}$) [c]	5 ($\times 10^{-10}$) [c]
MeOH	f_{obs}	4.01 ± 0.24	5.95 ± 0.30	2.71 ± 0.17	2.02 ± 0.17	2.13 ± 0.17
	f_{calc}	3.12	6.09	2.86	1.81	1.88
MeOD	f_{obs}	3.29 ± 0.17	2.90 ± 0.15	0.96 ± 0.21	–	–
	f_{calc}	1.80	2.36	0.78	0.37	0.29
EtOH	f_{obs}	3.26 ± 0.18	5.63 ± 0.29	2.53 ± 0.15	2.20 ± 0.31	1.92 ± 0.15
	f_{calc}	2.31	5.45	2.67	1.71	1.77
EtOD	f_{obs}	2.75 ± 0.16	2.50 ± 0.14	0.84 ± 0.11	–	–
	f_{calc}	1.35	2.12	0.74	0.35	0.27
1-PrOH	f_{obs}	3.15 ± 0.16	5.42 ± 0.28	2.34 ± 0.15	1.89 ± 0.17	1.84 ± 0.14
	f_{calc}	2.42	5.46	2.42	1.69	1.76
1-PrOD	f_{obs}	2.86 ± 0.15	2.54 ± 0.17	0.83 ± 0.12	–	–
	f_{calc}	1.41	2.12	0.73	0.34	0.27
2-PrOH	f_{obs}	2.35 ± 0.15	5.12 ± 0.26	2.32 ± 0.14	2.00 ± 0.19	1.93 ± 0.22
	f_{calc}	1.54	4.71	2.42	1.58	1.63
2-PrOD	f_{obs}	2.38 ± 0.12	2.40 ± 0.14	0.88 ± 0.06	–	–
	f_{calc}	0.91	1.83	0.67	0.32	0.25
t-BuOH	f_{obs}	1.87 ± 0.10	4.52 ± 0.23	2.30 ± 0.19	1.94 ± 0.22	1.64 ± 0.18
	f_{calc}	1.01	4.08	2.18	1.44	1.49
t-BuOD	f_{obs}	1.50 ± 0.11	2.25 ± 0.13	0.76 ± 0.09	–	–
	f_{calc}	0.61	1.59	0.60	0.29	0.23

[a] Experimental uncertainties are 95 % confidence intervals as discussed in the experimental section.
[b] Boltzmann distribution weighted sum of calculated oscillator strengths for individual conformers. Calculated using a 1D numerical local mode model with energies and dipole moments calculated at the CCSD(T)/aug-cc-pVTZ level of theory
[c] Multiplier indicates the power of ten needed to multiply the values in the column with, i.e. the experimental oscillator strength for the fundamental OH stretching transition in methanol is $(4.01 \pm 0.24) \times 10^{-6}$
[d] Oscillator strengths and uncertainties for the non-deuterated alcohols taken from Ref [12].

The agreement between our experimental oscillator strengths and the oscillator strengths from Lange et al. [12] is good for the $\Delta v_{OH} = 1$ stretching transitions with all differences between the two sets of oscillator strengths being less than the experimental uncertainties. See section S8 and S17 in the SI for more details. For the $\Delta v_{OH} = 2$ stretching transitions, we find a factor of 2 discrepancy between our oscillator strengths for MeOH and *t*-BuOH and the oscillator strengths from Lange et al. [12]. For 1-PrOH and 2-PrOH the differences in oscillator strengths are within the experimental uncertainties. Furthermore, Lange et al. [12] found that the ordering of the oscillator strengths in this region is different than in the fundamental region with 1-PrOH and 2-PrOH having the highest oscillator strengths. We, on the other hand, find that the trend in oscillator strengths is maintained in this region. We have not been able to explain the discrepancy between the results from Lange et al. and ours, but we do note that the experimental trend of oscillator strengths we find in the $\Delta v_{OH} = 2$ region is similar to the trend in our calculated oscillator strengths. See S9 in the SI for a more detailed discussion.

The oscillator strengths of the $\Delta v_{OH} = 4$ stretching transitions have been determined by both Lange et al. [12] and Phillips et al. [11] with the latter being a preliminary study including only MeOH, EtOH and 2-PrOH. In Fig. 7 we compare our oscillator strengths of the $\Delta v_{OH} = 4$ stretching transitions to these previous results. Firstly, we note that the differences in oscillator strengths between Phillips et al. [11] and Lange et al. [12] are greater than the experimental uncertainties for the three alcohols. For MeOH, EtOH and 2-PrOH our results are between the results from Phillips et al. [11] and Lange et al. [12]. The differences between our oscillator strengths and the oscillator strengths from Lange et al. are less than 25% and generally within the uncertainties (with 1-PrOH being the only exception).

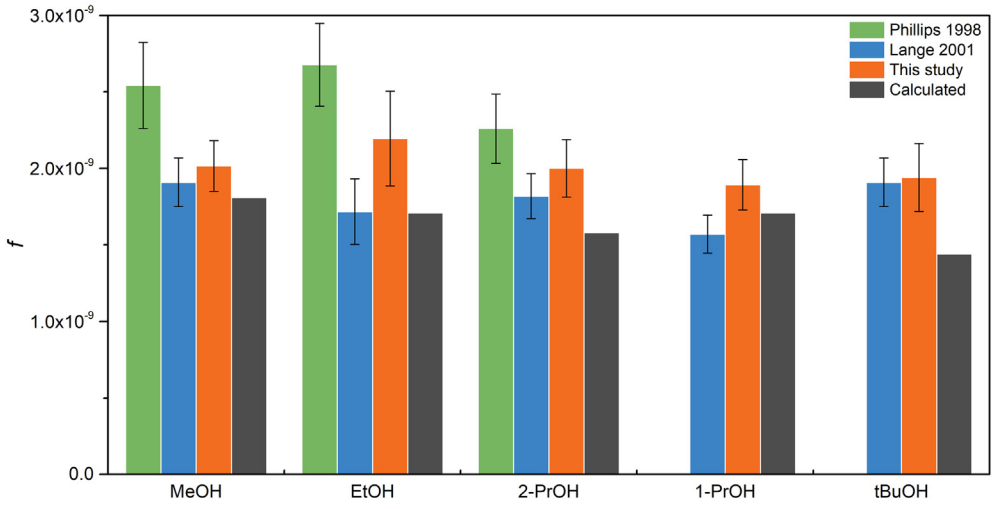

Fig. 7. Experimental and calculated oscillator strengths of the $\Delta v_{OH} = 4$ transitions compared to experimental oscillator strengths from Ref [11] and Ref [12].

The oscillator strengths for the $\Delta v_{OH} = 5$ stretching transitions have generally not been determined experimentally. The study from Phillips et al. [11] does, however, report an oscillator strength for the $\Delta v_{OH} = 5$ stretching transition in MeOH. Their spectra of MeOH used for the determination of the oscillator strength were recorded close to their detection limit and their experimental oscillator strength differs with almost a factor of 2 from our present results.

The calculated oscillator strengths are listed in Table 1. We find the biggest discrepancy between theory and experiment for the fundamental transitions. The oscillator strengths of the OH transitions are in better agreement with experiments than that of the OD transitions as expected due to the higher frequency of the OH stretching oscillator. This is not surprising as our 1D vibrational local mode model does not include the coupling to other vibrational modes that are important for describing the fundamental transitions.

For the $\Delta v_{OH} = 4 - 5$ transitions the calculated oscillator strengths are generally in good agreement with the experimental values, with differences less than 25%. This magnitude of discrepancy is similar to that found with CCSD(T)/aug-cc-pVTZ calculated oscillator strengths for diatomic molecules [28,58] and is an improvement compared to the 30–50 % differences found in previous studies of the third and fourth overtone transitions in polyatomic molecules in which the local mode vibrations were approximated as Morse oscillators [3,13,18,20,21]. We have tried using a Morse potential in our local mode calculations and in section S17 of the SI we show that the calculated oscillator strengths from this approach differ with ~50% from our experimental oscillator strengths. The similarity of the error in the calculated oscillator strengths for our study and for diatomic molecules (where the local mode model provides a full description of the vibrational picture) suggests that the source of the error in the calculations are the CCSD(T)/aug-cc-pVTZ calculated potential energy and dipole moment surfaces.

In the spectra of the $\Delta v_{OH} = 4 - 5$ transitions of EtOH and 2-PrOH, bands assigned to the two conformers are partly resolved. This allows us to experimentally estimate the Boltzmann distribution for these two compounds by comparing the measured and calculated band intensities. The entire overtone band is separated into two parts primarily belonging to each of the conformers and we integrate those parts separately as indicated in Fig. 8. By combining the ratio of the integrated absorbances for the *trans* and *gauche* parts of the band with calculated oscillator strength of the two conformers we can calculate a Boltzmann distribution from:

$$\frac{N_{trans}}{N_{gauche}} = \left(\frac{\int \alpha_{CRD}(\tilde{\nu})d\tilde{\nu}}{f_{calc}}\right)_{trans} \times \left(\frac{f_{calc}}{\int \alpha_{CRD}(\tilde{\nu})d\tilde{\nu}}\right)_{gauche} = \frac{g_{trans}}{g_{gauche}} \times \exp\left(\frac{-\Delta G^{\ominus}}{kT}\right), \quad (8)$$

where g is the degeneracy and $\Delta G^{\ominus}$ is the difference in Gibbs energy between the two conformers. A similar method has been used in a previous study [29]. For both EtOH and 2-PrOH we find that the *gauche* conformer is more abundant than the *trans* conformer with abundances of 56% and 72%, respectively, in agreement with our calculated Boltzmann distributions. These Boltzmann distributions correspond to differences in Gibbs energy of 91–92 cm^{-1} for EtOH and 56–64 cm^{-1} for 2-PrOH using the spectra of either the $\Delta v_{OH} = 4$ or the $\Delta v_{OH} = 5$ stretching transitions, respectively, which compares well with other literature values [46-50] and our calculated values of 50 and 70 cm^{-1}, respectively.

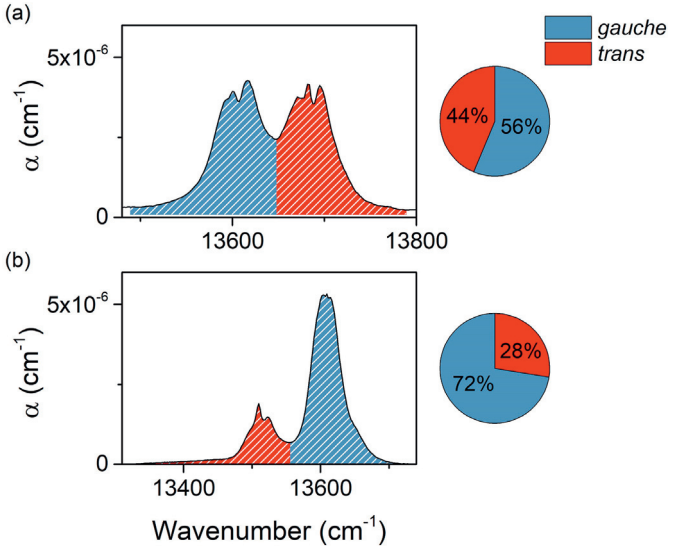

Fig. 8. Overtone spectra used for determining the Boltzmann distribution of the two conformers in (a) Ethanol and (b) 2-Propanol.

5. Conclusion

We have determined experimental oscillator strengths of the $\Delta v_{OH} = 1 - 2$ and $\Delta v_{OD} = 1 - 3$ in a range of simple alcohols using conventional FTIR spectroscopy. We found that the OH stretching transitions are more intense than the corresponding OD stretching transitions and that the f_{OH}/f_{OD} ratio increases with Δv. Furthermore, we have determined experimental oscillator strengths of the $\Delta v_{OH} = 4 - 5$ transitions using our newly constructed integrated CRD/FTIR flow setup. The agreement between our experimental oscillator strengths and the oscillator strengths determined by Lange et al. [12] and Phillips et al. [11] (using conventional spectroscopy) for the third overtone OH-stretching transitions shows that our CRD/FTIR flow cell setup gives reliable results. With the use of numerical 1D local mode theory combined with potential energies and dipole moments calculated at the CCSD(T)/aug-cc-pVTZ level of theory, we obtain oscillator strengths that are accurate (within 25%) compared to the experimental oscillator strength. Accurate experimental oscillator strengths are important for benchmarking theoretical studies and we hope that our experimentally determined oscillator strengths can provide a basis for future theoretical studies aimed at predicting absolute intensities for atmospherically relevant species.

Acknowledgements

We thank Veronica Vaida, Steven S. Brown, Kasper Mackeprang and Paul O. Wennberg for their helpful discussions. We thank the Danish Center for Scientific Computing and the Center for Exploitation of Solar Energy at the University of Copenhagen for the financial support.

Appendix A. Supplementary data

Supplementary data to this article can be found online at https://doi.org/10.1016/j.saa.2018.09.046.

References

[1] V. Vaida, H.G. Kjaergaard, P.E. Hintze, D.J. Donaldson, Photolysis of sulfuric acid vapor by visible solar radiation, Science 299 (5612) (2003) 1566–1568.
[2] P.E. Hintze, H.G. Kjaergaard, V. Vaida, J.B. Burkholder, Vibrational and electronic spectroscopy of sulfuric acid vapor, J. Phys. Chem. A 107 (8) (2003) 1112–1118.
[3] K.J. Feierabend, D.K. Havey, S.S. Brown, V. Vaida, Experimental absolute intensities of the $4\nu_9$ and $5\nu_9$ O-H stretching overtones of H_2SO_4, Chem. Phys. Lett. 420 (4) (2006) 438–442.

[4] P.O. Wennberg, R.J. Salawitch, D.J. Donaldson, T.F. Hanisco, E.J. Lanzendorf, K.K. Perkins, S.A. Lloyd, V. Vaida, R.S. Gao, E.J. Hintsa, R.C. Cohen, W.H. Swartz, T.L. Kusterer, D.E. Anderson, Twilight observations suggest unknown sources of HO_x, Geophys. Res. Lett. 26 (10) (1999) 1373–1376.
[5] H. Zhang, C.M. Roehl, S.P. Sander, P.O. Wennberg, Intensity of the second and third OH overtones of H_2O_2, HNO_3, and HO_2NO_2, J. Geophys. Res. 105 (D11) (2000) 14593–14598.
[6] B.G. Saar, A.H. Steeves, J.W. Thoman, D.L. Howard, D.P. Schofield, H.G. Kjaergaard, CH-stretching overtone spectroscopy of 1,1,1,2-tetrafluoroethane, J. Phys. Chem. A 109 (24) (2005) 5323–5331.
[7] S.S. Brown, R.W. Wilson, A.R. Ravishankara, Absolute intensities for third and fourth overtone absorptions in HNO_3 and H_2O_2 measured by cavity ring down spectroscopy, J. Phys. Chem. A 104 (21) (2000) 4976–4983.
[8] J.S. Wong, C.B. Moore, Inequivalent C-H oscillators of gaseous alkanes and alkenes in laser photoacoustic overtone spectroscopy, J. Chem. Phys. 77 (2) (1982) 603–615.
[9] A. Amrein, H.-R. Dübal, M. Lewerenz, M. Quack, Group additivity and overtone intensities for the isolated CH chromophore, Chem. Phys. Lett. 112 (5) (1984) 387–392.
[10] M. Lewerenz, M. Quack, Vibrational overtone intensities of the isolated CH and CD chromophores in fluoroform and chloroform, Chem. Phys. Lett. 123 (3) (1986) 197–202.
[11] J.A. Phillips, J.J. Orlando, G.S. Tyndall, V. Vaida, Integrated intensities of OH vibrational overtones in alcohols, Chem. Phys. Lett. 296 (3) (1998) 377–383.
[12] K.R. Lange, N.P. Wells, K.S. Plegge, J.A. Phillips, Integrated intensities of O-H stretching bands: fundamentals and overtones in vapor-phase alcohols and acids, J. Phys. Chem. A 105 (14) (2001) 3481–3486.
[13] S.D. Schrøder, A.S. Hansen, J.H. Wallberg, A.R. Nielsen, L. Du, H.G. Kjaergaard, The weak fundamental NH-stretching transition in amines, Spectrochim. Acta A 173 (2017) 201–206.
[14] H.G. Kjaergaard, H. Yu, B.J. Schattka, B.R. Henry, A.W. Tarr, Intensities in local mode overtone spectra: propane, J. Chem. Phys. 93 (1990) 6239–6248.
[15] B.I. Niefer, H.G. Kjaergaard, B.R. Henry, Intensity of CH- and NH-stretching transitions in the overtone spectra of cyclopropylamine, J. Chem. Phys. 99 (8) (1993) 5682–5700.
[16] H.G. Kjaergaard, D.M. Turnbull, B.R. Henry, Intensities of CH- and CD-stretching overtones in 1,3-butadiene and 1,3-butadiene-d_6, J. Chem. Phys. 99 (12) (1993) 9438–9452.
[17] H.G. Kjaergaard, B.R. Henry, CH stretching overtone spectra and intensities of vapor phase naphthalene, J. Phys. Chem. 99 (3) (1995) 899–904.
[18] H.G. Kjaergaard, Calculated OH-Stretching vibrational transitions of the water-nitric acid complex, J. Phys. Chem. A 106 (12) (2002) 2979–2987.
[19] Z. Rong, B.R. Henry, T.W. Robinson, H.G. Kjaergaard, Absolute intensities of CH stretching overtones in alkenes, J. Phys. Chem. A 109 (6) (2005) 1033–1041.
[20] J.R. Lane, H.G. Kjaergaard, K.L. Plath, V. Vaida, Overtone spectroscopy of sulfonic acid derivatives, J. Phys. Chem. A 111 (25) (2007) 5434–5440.
[21] V. Vaida, K.J. Feierabend, N. Rontu, K. Takahashi, Sunlight-initiated photochemistry: excited vibrational states of atmospheric chromophores, Int. J. Photoenergy 2008 (2008) 1–13.
[22] B.J. Miller, L. Du, T.J. Steel, A.J. Paul, A.H. Södergren, J.R. Lane, B.R. Henry, H.G. Kjaergaard, Absolute intensities of NH-stretching transitions in dimethylamine and pyrrole, J. Phys. Chem. A 116 (1) (2012) 290–296.
[23] A.W. Tarr, F. Zerbetto, Absolute intensities of CH-stretching overtones in chloroform and deuterochloroform, Chem. Phys. Lett. 154 (3) (1989) 273–279.
[24] K.K. Lehmann, A.M. Smith, Where does overtone intensity come from? J. Chem. Phys. 93 (9) (1990) 6140–6147.
[25] H.G. Kjaergaard, B.R. Henry, H. Wei, S. Lefebvre, T. Carrington, O.S. Mortensen, M.L. Sage, Calculation of vibrational fundamental and overtone band intensities of H_2O, J. Chem. Phys. 100 (1994) 6229–6239.
[26] K. Takahashi, M. Sugawara, S. Yabushita, Theoretical analysis on the fundamental and overtone OH stretching spectra of several simple acids and alcohols, J. Phys. Chem. A 107 (50) (2003) 11092–11101.
[27] D.P. Schofield, J.R. Lane, H.G. Kjaergaard, Hydrogen bonded OH-stretching vibration in the water dimer, J. Phys. Chem. A 111 (4) (2007) 567–572.
[28] J.R. Lane, H.G. Kjaergaard, XH-stretching overtone transitions calculated using explicitly correlated coupled cluster methods, J. Chem. Phys. 132 (2010) 174304.
[29] T.N. Wassermann, M.A. Suhm, Ethanol monomers and dimers revisited: a Raman study of conformational preferences and argon nanocoating effects, J. Phys. Chem. A 114 (32) (2010) 8223–8233.
[30] A.S. Hansen, L. Du, H.G. Kjaergaard, Positively charged phosphorus as a hydrogen bond acceptor, J. Phys. Chem. Lett. 5 (23) (2014) 4225–4231.
[31] P. Atkins, R. Friedman, Molecular Quantum Mechanics, 5th ed. ed., Oxford University Press, New York, 2011.
[32] P. Zalicki, R.N. Zare, Cavity ring-down spectroscopy for quantitative absorption measurements, J. Chem. Phys. 102 (7) (1995) 2708–2717.
[33] G. Berden, R. Peeters, G. Meijer, Cavity ring-down spectroscopy: experimental schemes and applications, Int. Rev. Phys. Chem. 19 (4) (2000) 565–607.
[34] A. Yalin, R. Zare, Effect of laser lineshape on the quantitative analysis of cavity ring-down signals, Laser Phys. 12 (2002) 1065–1072.
[35] H. Fuchs, W.P. Dubé, B.M. Lerner, N.L. Wagner, E.J. Williams, S.S. Brown, A sensitive and versatile detector for atmospheric NO_2 and NO_x based on blue diode laser cavity ring-down spectroscopy, Environ. Sci. Technol. 43 (20) (2009) 7831–7836.
[36] S.S. Brown, Absorption spectroscopy in high-finesse cavities for atmospheric studies, Chem. Rev. 103 (12) (2003) 5219–5238.
[37] A.D. Becke, Density-functional thermochemistry. III. The role of exact exchange, J. Chem. Phys. 98 (1993) 5648–5652.
[38] C. Lee, W. Yang, R.G. Parr, Development of the Colle-Salvetti correlation-energy formula into a functional of the electron density, Phys. Rev. B 37 (1988) 785–789.
[39] T.H. Dunning, Jr, Gaussian basis sets for use in correlated molecular calculations. I. The atoms boron through neon and hydrogen, J. Chem. Phys. 90 (1989) 1007–1023.
[40] M.J. Frisch, G.W. Trucks, H.B. Schlegel, G.E. Scuseria, M.A. Robb, J.R. Cheeseman, G. Scalmani, V. Barone, G.A. Petersson, H. Nakatsuji, X. Li, M. Caricato, A. Marenich, J. Bloino, B.G. Janesko, R. Gomperts, B. Mennucci, H.P. Hratchian, J.V. Ortiz, A.F. Izmaylov, J.L. Sonnenberg, D. Williams-Young, F. Ding, F. Lipparini, F. Egidi, J. Goings, B. Peng, A. Petrone, T. Henderson, D. Ranasinghe, V.G. Zakrzewski, J. Gao, N. Rega, G. Zheng, W. Liang, M. Hada, M. Ehara, K. Toyota, R. Fukuda, J. Hasegawa, M. Ishida, T. Nakajima, Y. Honda, O. Kitao, H. Nakai, T. Vreven, K. Throssell, J.A. Montgomery, Jr, J.E. Peralta, F. Ogliaro, M. Bearpark, J.J. Heyd, E. Brothers, K.N. Kudin, V.N. Staroverov, T. Keith, R. Kobayashi, J. Normand, K. Raghavachari, A. Rendell, J.C. Burant, S.S. Iyengar, J. Tomasi, M. Cossi, J.M. Millam, M. Klene, C. Adamo, R. Cammi, J.W. Ochterski, R.L. Martin, K. Morokuma, O. Farkas, J.B. Foresman, D.J. Fox, Gaussian 09 Revision D.01, Gaussian Inc., Wallingford CT, 2009.
[41] K. Raghavachari, G.W. Trucks, J.A. Pople, M. Head-Gordon, A fifth-order perturbation comparison of electron correlation theories, Chem. Phys. Lett. 157 (1989) 479–483.
[42] K. Raghavachari, J.A. Pople, E.S. Replogle, M. Head-Gordon, Fifth order Moeller–Plesset perturbation theory: comparison of existing correlation methods and implementation of new methods correct to fifth order, J. Phys. Chem. 94 (1990) 5579–5586.
[43] H.-J. Werner, P.J. Knowles, G. Knizia, F.R. Manby, M. Schütz,, P. Celani, W. Györffy, D. Kats, T. Korona, R. Lindh, A. Mitrushenkov, G. Rauhut, K.R. Shamasundar, T.B. Adler, R.D. Amos, A. Bernhardsson, A. Berning, D.L. Cooper, M.J.O. Deegan, A.J. Dobbyn, F. Eckert, E. Goll, C. Hampel, A. Hesselmann, G. Hetzer, T. Hrenar, G. Jansen, C. Köppl, Y. Liu, A.W. Lloyd, R.A. Mata, A.J. May, S.J. McNicholas, W. Meyer, M.E. Mura, A. Nicklass, D.P. O'Neill, P. Palmieri, D. Peng, K. Pflüger, R. Pitzer, M. Reiher, T. Shiozaki, H. Stoll, A.J. Stone, R. Tarroni, T. Thorsteinsson, M. Wang, MOLPRO version 2012.1, a package of ab initio programs, 2012. http://www.molpro.net.
[44] R. Meyer, Trigonometric interpolation method for one-dimensional quantum-mechanical problems, J. Chem. Phys. 52 (4) (1970) 2053–2059.
[45] K. Mackeprang, H.G. Kjaergaard, Vibrational transitions in hydrogen bonded bimolecular complexes - a local mode perturbation theory approach to transition frequencies and intensities, J. Mol. Spec. 334 (2017) 1–9.
[46] J.R. Durig, W.E. Bucy, C.J. Wurrey, L.A. Carreira, Raman spectra of gases. XVI. Torsional transitions in ethanol and ethanethiol, J. Phys. Chem. 79 (10) (1975) 988–993.
[47] R.K. Kakar, C.R. Quade, Microwave rotational spectrum and internal rotation in gauche ethyl alcohol, J. Chem. Phys. 72 (8) (1980) 4300–4307.
[48] H.L. Fang, R.L. Swofford, Molecular conformers in gas-phase ethanol: a temperature study of vibrational overtones, Chem. Phys. Lett. 105 (1) (1984) 5–11.
[49] E. Hirota, Internal rotation in isopropyl alcohol studied by microwave spectroscopy, J. Phys. Chem. 83 (11) (1979) 1457–1465.
[50] A. Maeda, I.R. Medvedev, F.C.D. Lucia, E. Herbst, The millimeter- and submillimeter-wave spectrum of iso-propanol [$(CH_3)_2CHOH$], ApJS 166 (2) (2006) 650.
[51] H.L. Fang, D.M. Meister, R.L. Swofford, Photoacoustic spectroscopy of vibrational overtones in gas-phase CH_3OH and CH_3OD, J. Phys. Chem. 88 (3) (1984) 405–409.
[52] J.M. Jasinski, Fourth overtone spectra of OH Oscillators in simple alcohols, Chem. Phys. Lett. 109 (5) (1984) 462–467.
[53] H.L. Fang, D.A.C. Compton, Vibrational overtones of gaseous alcohols, J. Phys. Chem. 92 (23) (1988) 6518–6527.
[54] L. Lubich, O.V. Boyarkin, R.D.F. Settle, D.S. Perry, T.R. Rizzo, Multiple timescales in the intramolecular vibrational energy redistribution of highly excited methanol, Faraday Discuss. 102 (1995) 167–178.
[55] O.V. Boyarkin, L. Lubich, R.D.F. Settle, D.S. Perry, T.R. Rizzo, Intramolecular energy transfer in highly vibrationally excited methanol. I. Ultrafast dynamics, J. Chem. Phys. 107 (20) (1997) 8409–8422.
[56] J.D. Weibel, C.F. Jackels, R.L. Swofford, Experimental and ab initio investigation of the O-H overtone vibration in ethanol, J. Chem. Phys. 117 (9) (2002) 4245–4254.
[57] D.L. Howard, H.G. Kjaergaard, Resonance coupling in the fourth OH-stretching overtone spectrum of formic acid, J. Chem. Phys. 121 (1) (2004) 136–140.
[58] I. Gordon, L. Rothman, C. Hill, R. Kochanov, Y. Tan, P. Bernath, M. Birk, V. Boudon, A. Campargue, K. Chance, B. Drouin, J.-M. Flaud, R. Gamache, J. Hodges, D. Jacquemart, V. Perevalov, A. Perrin, K. Shine, M.-A. Smith, J. Tennyson, G. Toon, H. Tran, V. Tyuterev, A. Barbe, A. Csaszar, V. Devi, T. Furtenbacher, J. Harrison, J.-M. Hartmann, A. Jolly, T. Johnson, T. Karman, I. Kleiner, A. Kyuberis, J. Loos, O. Lyulin, S. Massie, S. Mikhailenko, N. Moazzen-Ahmadi, H. Müller, O. Naumenko, A. Nikitin, O. Polyansky, M. Rey, M. Rotger, S. Sharpe, K. Sung, E. Starikova, S. Tashkun, J.V. Auwera, G. Wagner, J. Wilzewski, P. Wcislo, S. Yu, E. Zak, The HITRAN2016 Molecular Spectroscopic Database, J. Quant. Spectrosc. Radiat. Transfer 203 (2017) 3–69.